Topochemical Synthesis of Three-Dimensional Perovskites from Lamellar Precursors

Raymond E. Schaak and Thomas E. Mallouk*

Contribution from the Department of Chemistry, The Pennsylvania State University, University Park, Pennsylvania 16802

Received September 13, 1999

Abstract: A topochemical route to nondefect, three-dimensional perovskites from lamellar Dion−Jacobson and Ruddlesden−Popper precursors was demonstrated. The method involves reduction of one of the ions (in this case Eu^{3+}) in the precursor phase and concomitant loss of oxygen. $CsEu_2Ti_2NbO_{10}$, a three-layer Dion−Jacobson compound, was ion-exchanged to $AEu_2Ti_2NbO_{10}$ (A = Na, Li) and reduced in hydrogen to form the $SrTiO_3$-type perovskites $AEu_2Ti_2NbO_9$. Similarly, $K_2Eu_2Ti_3O_{10}$, a three-layer Ruddlesden−Popper compound, underwent divalent ion exchange to form the Dion−Jacobson compounds $A^{II}Eu_2Ti_3O_{10}$ (A^{II} = Ca, Sr) and $M^{II}Eu_2Ti_3O_{10}$ (M^{II} = Ni, Cu, Zn), which were reduced in hydrogen to perovskite-type $A^{II}Eu_2Ti_3O_9$ and M^{II}-$Eu_2Ti_3O_9$, respectively. The A^{II} and Eu^{2+} ions of $A^{II}Eu_2Ti_3O_9$ remain ordered, while A-site disordering occurs in the other perovskites. In all cases, the anisotropic texture of the layered precursors is retained in the product perovskite phase.

Introduction

Perovskites are metal oxides of simplest formula ABO_3, in which B is a small transition metal ion and A is a larger cation of an s-, d-, or f-block element.[1] Stoichiometric and oxygen-deficient perovskites, as well as intergrowth compounds that contain alternating blocks of perovskite and other structures, are well-known for their interesting properties as dielectrics, ferroelectrics, high-Tc superconductors, colossal magnetoresistive materials, and catalysts.

Perovskites and other refractory metal oxides are normally prepared by high-temperature reactions of the appropriate mixture of oxides, carbonates, and/or nitrates. While this is a useful route to thermodynamically stable compounds, it does not in general allow fine control over the microscopic or macroscopic structural features of the product, or provide access to more complex metastable phases. Better synthetic control is needed to prepare, for example, magnetoresistive perovskites with ordering of different types of A and B ions,[2] intergrowth structures such as superconductors with specific sequences of CuO_2 sheets,[3] ferroelectric compounds with very anisotropic texture,[4] and photocatalysts that favor the separation of photogenerated electron−hole pairs over charge recombination.[5]

High temperatures are needed to drive most solid-state reactions because diffusion is rate-limiting. Alternative strategies that sidestep the diffusion limitation open the door to a wider variety of solids made by design. These include thin film methods, such as evaporation,[6] pulsed laser deposition,[7] electrodeposition,[8] and molecular beam epitaxy.[9] "Soft" solid-state reactions, on the other hand, overcome the diffusion problem in bulk syntheses by making use of precursors that already contain most of the bonds of the desired product.[10] Familiar examples are the intercalation reactions of lamellar compounds and ion exchange reactions of open-framework solids such as zeolites.

A less common but very attractive technique from the point of view of rational materials synthesis is the topochemical transformation of a lamellar solid into a three-dimensional product phase. Topochemical reactions have now been used successfully in a few such systems to obtain metastable compounds that are inaccessible by other techniques. The synthesis of $Ti_2Nb_2O_9$ from $HTiNbO_5$,[11] the topochemical

(1) Galasso, F. S. *Structure, Properties and Preparation of Perovskite-type Compounds*; Pergamon Press: Oxford, 1969.

(2) Moritomo, Y.; Asamitsu, A.; Kuwahara, H.; Tokura, Y. *Nature* **1996**, *380*, 141.

(3) (a) Otzschi, K. D.; Poeppelmeier, K. R.; Salvador, P. A.; Mason, T. O.; Zhang, H.; Marks, L. D. *J. Am. Chem. Soc.* **1996**, *118*, 8951. (b) Salvador, P. A.; Greenwod, K. B.; Mawdsley, J. R.; Poeppelmeier, K. R.; Mason, T. O. *Chem. Mater.* **1999**, *11*, 1760.

(4) (a) Brahmaroutu, B.; Messing, G. L.; Trolier-McKinstry, S.; Selvaraj, U. *Proceedings of the 10th IEEE International Symposium on Applications of Ferroelectrics*; Kulwicki, B. M.; Amin, A.; Safari, A., IEEE, Piscataway, NJ, 1996; Vol. II, pp 883−886. (b) Seabaugh, M.; Hong, S.-H.; Messing, G. L. In *Ceramic Microstructure: Control at the Atomic Level*; Tomsia, A. P., Glaeser, A., Eds.; Plenum Press: New York, 1998; pp 303−310. (c) Takeuchi, T.; Tani, T.; Satoh, T. *Solid State Ionics* **1998**, *108*, 67. (d) Tani, T. *J. Korean Phys. Soc.* **1998**, *32*, S1217. (e) Horn, J.; Zhang, S. C.; Selvaraj, U.; Messing, G. L.; Trolier-McKinstry, S. *J. Am. Ceram. Soc.* **1999**, *82*, 921. (f) Rehrig, P. W.; Park, S.-E.; Trolier-McKinstry, S.; Messing, G. L.; Jones, B.; Shrout, T. R. *J. Appl. Phys.* **1999**, *86*, 1657.

(5) (a) Takata, T.; Furumi, Y.; Shinohara, K.; Tanaka, A.; Hara, M.; Kondo, J. N.; Domen, K. *Chem. Mater.* **1997**, *9*, 1063. (b) Kim, H. G.; Hwang, D. W.; Kim, J.; Kim, Y. G.; Lee, J. S. *Chem. Commun.* **1999**, 1077.

(6) (a) Novet, T.; Johnson, D. C. *J. Am. Chem. Soc.* **1991**, *113*, 3398. (b) Novet, T.; McConnell, J. M.; Johnson, D. C. *Chem. Mater.* **1992**, *4*, 473. (c) Fister, L.; Johnson, D. C. *J. Am. Chem. Soc.* **1992**, *114*, 4639. (d) Xu, Z.; Tang, Z.; Devan, S. D.; Novet, T.; Johnson, D. C. *J. Appl. Phys.* **1993**, *74*, 905. (e) Sellinschegg, H.; Stuckmeyer, S. L.; Hornbostsel, M. D.; Johnson, D. C. *Chem. Mater.* **1998**, *10*, 1096. (f) Schneidmiller, R.; Bentley, A.; Hornbostel, M. D.; Johnson, D. C. *J. Am. Chem. Soc.* **1999**, *121*, 3142.

(7) Lowndes, D. H.; Geohegan, D. B.; Puretzky, A. A.; Norton, D. P.; Rouleau, C. M. *Science* **1996**, *273*, 898.

(8) Switzer, J. A.; Shumsky, M. G.; Bohannan, E. W. *Science* **1999**, *284*, 293.

(9) (a) Theis, D.; Yeh, J.; Schlom, D. G.; Hawley, M. E.; Brown, G. W.; Jiang, J. C.; Pan, X. Q. *Appl. Phys. Lett.* **1998**, *72*, 2817. (b) Lettieri, J.; Jia, Y.; Urbanik, M.; Weber, C. I.; Maria, J.-P.; Schlom, D. G.; Li, H.; Ramesh, R.; Uecker, R.; Reiche, P. *Appl. Phys. Lett.* **1998**, *73*, 2923.

(10) (a) Rao, C. N. R.; Gopalakrishnan, J. In *New Directions in Solid State Chemistry*, 2nd ed.; Cambridge University Press: Cambridge, 1997. (b) Stein, A.; Keller, S. W.; Mallouk, T. E. *Science* **1993**, *259*, 1558.

10.1021/ja993306i CCC: $19.00
Published on Web 03/09/2000

reduction of $LiVMoO_6$ brannerites to form $LiVMoO_5$,[12] and the syntheses of hexagonal WO_3 from $WO_3 \cdot {}^1/_3H_2O$ and ReO_3-type MoO_3 from $MoO_3 \cdot {}^1/_3H_2O$[13] serve as important examples. Among the perovskite family of transition-metal oxides, topochemical reactions have been used to make novel cation-deficient metastable phases such as $La_{2/3}TiO_3$,[14] $Nd_2Ti_3O_9$,[15] $SrTa_{2-x}Nb_xO_6$,[16] and $Ca_4Nb_6O_{19}$.[17] Currently, the only routes available to transform layered perovskites into metastable three-dimensional phases involve either a dehydration mechanism,[14,16] which inevitably leaves a cation deficiency on the A site, or high-pressure techniques, which require low coordination numbers[18] or anion deficiency[19] in the lamellar precursor.

Members of the Dion−Jacobson family of layered perovskites,[20] $A[A_{n-1}'B_nO_{3n+1}]$ (A = alkali, A′ = alkaline earth or rare earth, B = transition metal), have an equal number of A(A′) and B cations, so they are ideal precursors to nondefective, three-dimensional perovskites of the general formula $AA_{n-1}'B_nO_{3n}$. Recent examples[21] of divalent ion exchange in the Ruddlesden−Popper series of layered perovskites,[22] $A_2[A_{n-1}'B_nO_{3n+1}]$, provide an even wider choice of stoichiometric Dion−Jacobson precursors to three-dimensional perovskites. A method for transforming these lamellar compounds into extended perovskites could take advantage of the composition and stacking sequence of the precursor layers to access particular structures and properties. Since methods already exist for chemically "peeling" Dion−Jacobson phases apart into single sheets[23] and restacking them in any desired sequence on a surface,[24] in principle one might design and synthesize a very rich variety of new perovskites in this way as thin films. We describe here a first step toward this goal, which is a new topochemical reduction reaction that transforms Dion−Jacobson precursors into nondefective three-dimensional perovskites.

Experimental Section

Synthesis. $K_2Eu_2Ti_3O_{10}$ and $CsEu_2Ti_2NbO_{10}$ were prepared by the solid-state reactions of stoichiometric amounts of A_2CO_3, Eu_2O_3, TiO_2, and Nb_2O_5 at 1050 °C for 1 day. A 40% molar excess of A_2CO_3 was added to compensate for loss due to volatilization. $A^{II}Eu_2Ti_3O_{10}$ (A^{II} = Ca, Sr) and $M^{II}Eu_2Ti_3O_{10}$ (M^{II} = Ni, Cu, and Zn) were prepared by ion-exchanging 1 g of $K_2Eu_2Ti_3O_{10}$ in 100 mL of 1 M aqueous solutions of the appropriate nitrate salts. The ion-exchange reactions were accomplished by stirring the mixture at 40 °C for 8 days. $ZnEu_2Ti_3O_{10}$ was also prepared by ion-exchanging $K_2Eu_2Ti_3O_{10}$ in molten $ZnCl_2$ at 300 °C for 2 weeks.[21a] $AEu_2Ti_2NbO_{10}$ (A = Na, Li) compounds were prepared by ion-exchanging $CsEu_2Ti_2NbO_{10}$ in the molten alkali nitrates at 350 °C for 2 weeks. All ion-exchange solutions and molten salts were replaced every 2 days to ensure full exchange, and all products were washed thoroughly with deionized, distilled water. $ZnEu_2Ti_3O_{10}$ prepared using $ZnCl_2$ was also washed with dilute HNO_3 to remove a ZnO impurity. The completeness of each ion-exchange reaction was estimated by energy-dispersive X-ray emission analysis (EDAX) and by phase purity as evidenced by powder X-ray diffraction (XRD). The ion-exchanged precursors were reduced in flowing H_2 at 650 to 850 °C for 6 to 12 h. Additionally, all $AEu_2Ti_2NbO_9$, $A^{II}Eu_2Ti_3O_9$, and $M^{II}Eu_2Ti_3O_9$ compounds were synthesized directly from the corresponding oxides and carbonates in flowing H_2 at 1000 °C for 1 day.

X-ray Diffraction. X-ray diffraction (XRD) patterns were obtained on a Phillips X'Pert MPD diffractometer using monochromatized Cu Kα (λ = 1.5418 Å) radiation. Diffraction patterns from powdered samples held on a quartz zero background plate were obtained in $\theta-\theta$ geometry. Lattice parameters and atomic positions of precursor and product phases were determined by the Rietveld method using the GSAS structure refinement package.[25]

Scanning Electron Microscopy. SEM images were recorded at the Electron Microscope Facility for the Life Sciences in the Biotechnology Institute at the Pennsylvania State University, using a JEOL-JSM 5400 microscope at 30 kV accelerating voltage. Prior to imaging, the samples were affixed to double sticky carbon tabs and sputter coated with 10 nm of Au/Pd in a BAL-TEC SCD050 sputter-coater.

Results and Discussion

Topochemical Reduction of Dion−Jacobson Phases to Perovskites. The conversion of a Dion−Jacobson phase $A[A_{n-1}'B_nO_{3n+1}]$ to a perovskite $AA_{n-1}'B_nO_{3n}$ requires that either the A, A′, or B ion be reducible. While many of the interesting product phases are B-site mixed valence compounds (for example, $Mn^{3+/4+}$ magnetoresistive materials and $Cu^{2+/3+}$ superconductors), for proof-of-concept purposes we have used Eu^{3+} as an easily reduced A′ site cation. When a Dion−Jacobson phase $AEu_2B_3O_{10}$ is heated in hydrogen, Eu^{3+} is reduced to Eu^{2+}, and the concomitant release of water creates oxygen vacancies within the lattice. If the oxygen vacancies order along the interlayer gallery, a topochemical collapse of the layered structure is possible, with the BO_6 octahedra of the $[A_{n-1}'B_nO_{3n}]$ perovskite blocks encasing the A ions in the interlayer gallery. The idealized topochemical mechanism is sketched in Figure 1.

Synthesis and Structure of Dion−Jacobson Precursors and Perovskites. $AEu_2Ti_2NbO_{10}$ compounds of the lighter alkali metals (A = Na, Li) adopt a three-dimensional structure when synthesized directly, so $CsEu_2Ti_2NbO_{10}$ (Figure 2a) was prepared as the Dion−Jacobson phase precursor to these compounds. Layered perovskite phases provide large sites for interlayer cations, so the use of Cs favors these structures, as previously noted for the $ASrLaNb_2M^{II}O_9$ series.[26] For the same reason, Cs is too large to fit into the A site of a three-dimensional perovskite. The Li and Na (Figure 2b) forms of $AEu_2Ti_2NbO_{10}$ were accessed by ion exchange of the Cs compound in the molten alkali nitrates. EDAX confirmed the removal of Cs from

(11) Rebbah, H.; Desgardin, G.; Raveau, B. *Mater. Res. Bull.* **1979**, *14*, 1125.
(12) Gopalakrishnan, J.; Bhuvanesh, N. S. P.; Vijayaraghavan, R.; Vasanthacharya, N. Y. *J. Mater. Chem.* **1997**, *7*, 307.
(13) (a) Figlarz, M. *Prog. Solid State Chem.* **1989**, *19*, 1. (b) McCarron, E. M. *J. Chem. Soc., Chem. Commun.* **1986**, 336.
(14) Gopalakrishnan, J.; Bhat, V. *Inorg. Chem.* **1987**, *26*, 4301.
(15) Dulieu, B.; Bullot, J.; Wery, J.; Richard, M.; Brohan, L. *Phys. Rev. B* **1996**, *53*, 10641.
(16) Ollivier, P. J.; Mallouk, T. E. *Chem. Mater.* **1998**, *10*, 2585.
(17) Fang, M.; Kim, C. H.; Mallouk, T. E. *Chem. Mater.* **1999**, *11*, 1519.
(18) Vander Griend, D. A.; Boudin, S.; Poeppelmeier, K. R.; Azuma, M.; Toganoh, H.; Takano, M. *J. Am. Chem. Soc.* **1998**, *120*, 11518.
(19) Byeon, S.; Kim, H.; Yoon, J.; Dong, Y.; Yun, H.; Inaguma, Y.; Itoh, M. *Chem. Mater.* **1998**, *10*, 2317.
(20) (a) Dion, M.; Ganne, M.; Tournoux, M. *Mater. Res. Bull.* **1981**, *16*, 1429. (b) Jacobson, A. J.; Johnson, J. W.; Lewandowski, J. T. *Inorg. Chem.* **1985**, *24*, 3727. (c) Treacy, M. M. J.; Rice, S. B.; Jacobson, A. J.; Lewandowski, J. T. *Chem. Mater.* **1990**, *2*, 279.
(21) (a) Hyeon, K.; Byeon, S. *Chem. Mater.* **1999**, *11*, 352. (b) McIntyre, R. A.; Falster, A. U.; Li, S.; Simmons, W. B., Jr.; O'Connor, C. J.; Wiley, J. B. *J. Am. Chem. Soc.* **1998**, *120*, 217. (c) Lalena, J. N.; Cushing, B. L.; Falster, A. U.; Simmons, W. B., Jr.; Seip, C. T.; Carpenter, E. E.; O'Connor, C. J.; Wiley, J. B. *Inorg. Chem.* **1998**, *37*, 4484. (d) Mahler, C. H.; Cushing, B. L.; Lalena, J. N.; Wiley, J. B. *Mater. Res. Bull.* **1998**, *33*, 1581. (e) Cushing, B. L.; Wiley, J. B. *Mater. Res. Bull.* **1999**, *34*, 271.
(22) (a) Ruddlesden, S. N.; Popper, P. *Acta Crystallogr.* **1957**, *10*, 538; Ruddlesden, S. N.; Popper, P. *Acta Cystallogr.* **1958**, *11*, 54. (b) Uma, S.; Raju, A. R.; Gopalakrishnan, J. *J. Mater. Chem.* **1993**, *3*, 709.
(23) (a) Jacobson, A. J. *Mater. Sci. Forum* **1994**, 152−153, 1. (b) Jacobson, A. J. In *Comprehensive Supramolecular Chemistry*; Alberti, G., Bein, T., Eds.; Elsevier: Oxford, UK, 1996; Vol. 7, pp 315−335.
(24) Fang, M.; Kim, H. N.; Saupe, G. B.; Miwa, T.; Fujishima, A.; Mallouk, T. E. *Chem. Mater.* **1999**, *11*, 1526.
(25) (a) Rietveld, H. M. *J. Appl. Crystallogr.* **1969**, *2*, 65. (b) Larson, A. C.; von Dreele, R. B. *Program version: PC-98*; Los Alamos National Lab. Rep. No. LA-UR-86-748, 1994.
(26) Gopalakrishnan, J.; Uma, S.; Vasanthacharya, N. Y.; Subbanna, G. N. *J. Am. Chem. Soc.* **1995**, *117*, 2353.

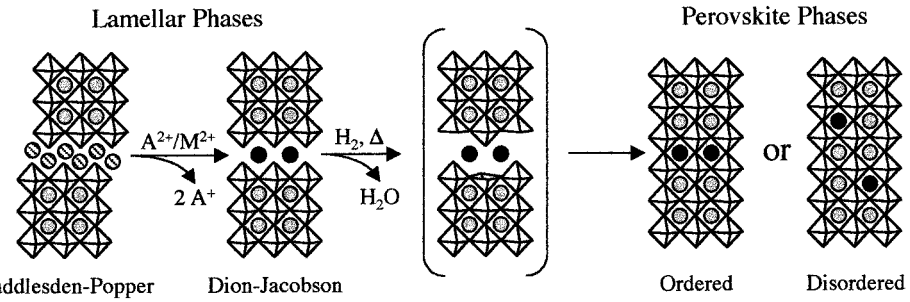

Figure 1. Topochemical transformation from a layered to a three-dimensional perovskite. The octahedra represent MO_6 units, the gray circles represent Eu, and the hatched and solid circles represent A^+, A^{2+}, or M^{2+}.

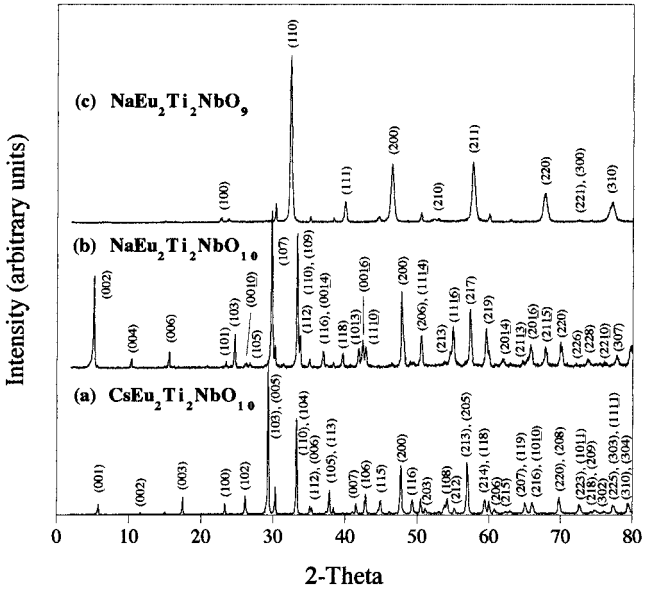

Figure 2. XRD patterns for (a) $CsEu_2Ti_2NbO_{10}$, (b) $NaEu_2Ti_2NbO_{10}\cdot xH_2O$, and (c) $NaEu_2Ti_2NbO_9$. Unindexed peaks represent a pyrochlore impurity phase.

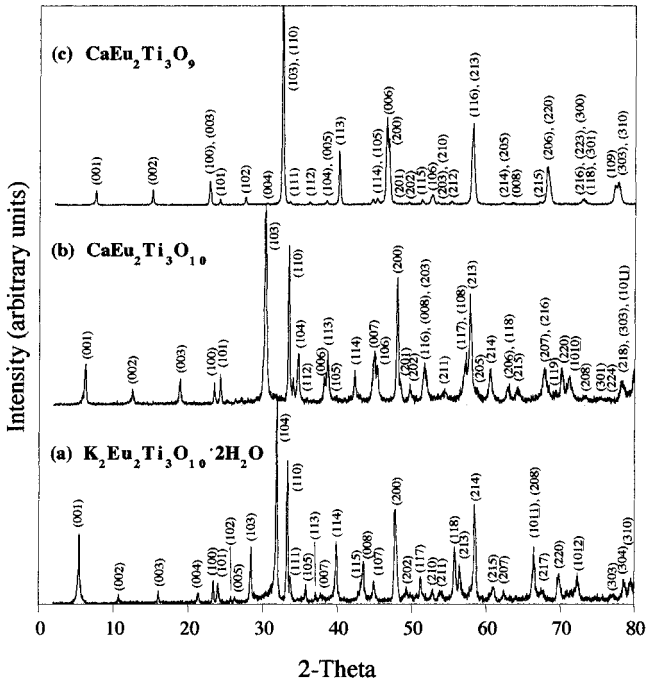

Figure 3. XRD patterns for (a) $K_2Eu_2Ti_3O_{10}\cdot 2H_2O$, (b) $CaEu_2Ti_3O_{10}$, and (c) $CaEu_2Ti_3O_9$.

the precursor. Since the ratio of Eu to Ti in $AEu_2Ti_2NbO_{10}$ is 1:1, the stable pyrochlore phase $Eu_2Ti_2O_7$ also forms readily and could not be avoided as an impurity. The pyrochlore phase remained unchanged during both the ion exchange of the Dion−Jacobson phase and the hydrogen reduction of the Dion−Jacobson phase to perovskite $AEu_2Ti_2NbO_9$.

$AEu_2Ti_2NbO_9$ (A = Na, Li) forms a $SrTiO_3$-type cubic perovskite (Figure 2c). The absence of layer lines in the X-ray diffraction pattern indicates disorder of the alkali and Eu ions among the available A sites of the perovskite lattice. Both Na and Li are monovalent and sufficiently small that the high temperature of the reduction reaction allows them to move in the perovskite lattice. Similar disordering of A-site cations occurs in the lower temperature topochemical synthesis of cation-deficient perovskites $SrTa_{2-x}Nb_xO_6$ from $H_2SrTa_{2-x}Nb_xO_7$.[16]

Conversion of Ruddlesden−Popper Precursors to Perovskites. The $n = 3$ Ruddlesden−Popper phase $K_2Eu_2Ti_3O_{10}$ hydrates immediately upon exposure to air, so the hydrate $K_2Eu_2Ti_3O_{10}\cdot 2H_2O$, which is structurally identical to $K_2La_2Ti_3O_{10}\cdot 2H_2O$,[14,27] was used (Figure 3a). Divalent ion-exchange in Ruddlesden−Popper phases has recently been studied,[21] and most exchanges have been carried out by heating an intimate mixture of the lamellar precursor and the anhydrous alkaline earth nitrate in a sealed tube. In all cases, these exchanges are incomplete. In our hands, exchange in aqueous solutions of the nitrates was equally effective, although as in the solid-state reaction some of the precursor phase remained unchanged. The exchange products $A^{II}Eu_2Ti_3O_{10}$ (A^{II} = Ca, Sr) and $M^{II}Eu_2Ti_3O_{10}$ (M^{II} = Ni, Cu, Zn) were dried at 400 °C to remove interlayer water, and the resulting XRD patterns matched those predicted for the anhydrous phases. The EDAX data shown in Table 1 indicate that approximately 70 to 85% of the interlayer potassium ions were removed by the aqueous ion exchange, which is consistent with the exchange efficiencies obtained using the anhydrous nitrates.[21b−e] $ZnEu_2Ti_3O_{10}$ was also prepared with a similar exchange efficiency using molten $ZnCl_2$ as the exchange salt.[21a]

Table 1. EDAX Results for Divalent Ion Exchange

compound	% K^+ exchanged[a]
$CaEu_2Ti_3O_{10}$	80
$SrEu_2Ti_3O_{10}$	76
$NiEu_2Ti_3O_{10}$	75
$CuEu_2Ti_3O_{10}$	70
$ZnEu_2Ti_3O_{10}$ (aq)	68
$ZnEu_2Ti_3O_{10}$ ($ZnCl_2$)	78

[a] Percent exchange is based on an analysis of the remaining K^+.

$A^{II}Eu_2Ti_3O_9$ (A^{II} = Ca, Sr) also has an $SrTiO_3$-type perovskite structure, but the presence of low-angle reflections in Figure 3c indicates that the alkaline earth and Eu ions remain ordered

(27) Toda, K.; Watanabe, J.; Sato, M. *Mater. Res. Bull.* **1996**, *31*, 1427.

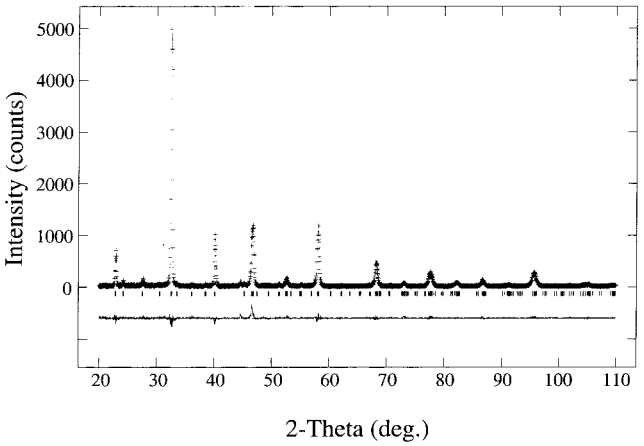

Figure 4. Structure refinement (GSAS) for the cation-ordered perovskite phase $SrEu_2Ti_3O_9$, showing calculated (top, solid line) and observed (top, crosses) XRD patterns. The difference curve (bottom, solid line) indicates the agreement between the observed and calculated patterns. Bragg reflections are indicated by the tick marks below the peaks.

in separate layers. The XRD pattern for $SrEu_2Ti_3O_9$ was simulated (Figure 4), and atomic positions refined well ($R_f^2 = 0.1068$)[28] on the basis of an ordered tetragonal structure with $c/a = 3.015$. Similar results were obtained with A = Ca ($c/a = 3.016$). Apparently, the charge and size of the divalent ions A^{2+} and Eu^{2+} provide a sufficient barrier to disordering. The cation ordering provides good evidence that the reaction is topochemical, since the direct synthesis of $A^{II}Eu_2Ti_3O_9$ from the oxides and carbonates under hydrogen produces a mixture of phases, including the $SrTiO_3$-type cubic perovskite with the alkaline earth and Eu ions disordered among the A sites. It is worth noting that the ordered $A^{II}Eu_2Ti_3O_9$ (A^{II} = Ca, Sr) phases were formed from the $A^{II}Eu_2Ti_3O_{10}$ precursors within 1 h of reduction in hydrogen at 750 °C. Such a rapid synthesis is consistent with a topochemical mechanism.

Similar reductive syntheses of $M^{II}Eu_2Ti_3O_9$ (M^{II} = Ni, Cu, Zn) from Dion−Jacobson $M^{II}Eu_2Ti_3O_{10}$ precursors provide some insight into the topochemical mechanism of the reduction reaction. The progression of phases formed in this reaction is shown by the XRD patterns in Figure 5. In the initial stages of the reaction of the Zn compound, carried out at 650 °C, the white precursor $ZnEu_2Ti_3O_{10}$ changes gradually in color from white to gray to black. After 8 h, the XRD pattern in Figure 5b is obtained. This pattern can be indexed to a mixture of layered tetragonal phases, one with $a = 3.809$, $c = 27.544$, and the other with $a = 3.885$, $c = 12.131$. The former has slightly larger *a*-axis and *c*-axis spacings than the precursor Dion−Jacobson phase ($a = 3.7729$, $c = 27.09$). The *a*-axis (in-plane) expansion suggests that the new phase is an intermediate containing reduced Eu^{2+} ions, which are larger than Eu^{3+} ions. Interestingly, the larger *c*-axis value is consistent with the larger size of Eu^{2+}, and also possibly reflects the introduction of hydrogen prior to the collapse shown schematically in Figure 1. The second phase is the fully collapsed perovskite compound $ZnEu_2Ti_3O_9$, which has partial disorder of divalent Zn and Eu A-site cations. Further heating yields the fully disordered cubic perovskite, as shown by the XRD pattern in Figure 5c. The appearance of intermediate ordered phases on the way to the thermodynamically stable disordered perovskite, which is also

(28) The structure of $SrEu_2Ti_3O_9$ was refined (GSAS) using an ordered tetragonal unit cell belonging to space group *P*4*mm*. Structural and profile parameters were refined to convergence that led to $R_f^2 = 0.1068$, $R_p = 0.1426$, and $R_{wp} = 0.2178$.

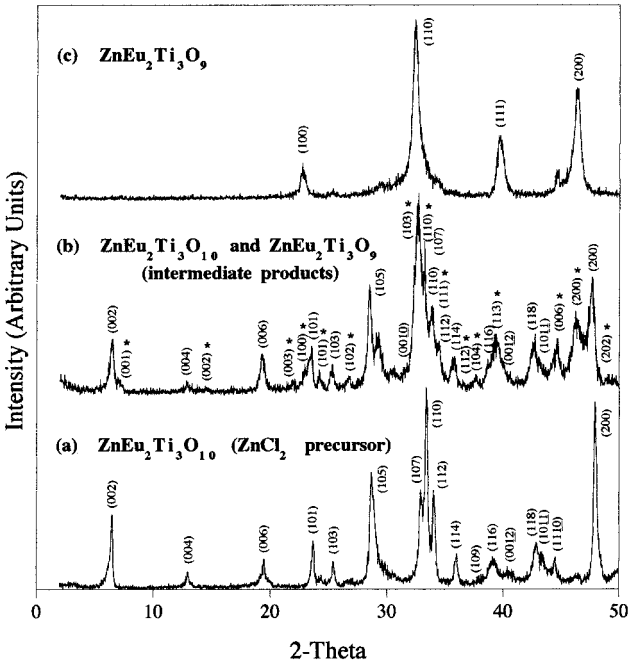

Figure 5. XRD patterns for (a) $ZnEu_2Ti_3O_{10}$ prepared from the $ZnCl_2$ precursor, (b) the intermediate products made by heating this compound in H_2 at 650 °C for 8 h, and (c) the cation-disordered perovskite $ZnEu_2Ti_3O_9$ obtained after heating in H_2 at 850 °C for 4 h. In panel b, indexing for the ordered three-dimensional phase is indicated by asterisks.

the product of direct synthesis under hydrogen, argues strongly that the reduction reaction is topochemical. Similar cubic phases were the ultimate products with M^{II} = Ni and Cu. No metallic Ni or Cu was detected by XRD of the reduced phases, so decomposition to a zerovalent metal dispersed on a defect $Eu_{2/3}TiO_3$ perovskite is unlikely. However, a detailed electron microscopy study is necessary to unambiguously characterize the samples.

Since the divalent ion exchanges are not stoichiometric, the unexchanged potassium must be accounted for in the reduced phases. One possibility is that potassium and europium are mixed on the A and A′ sites, such that even full exchange leaves some potassium in the perovskite block. However, no Eu^{3+} was detected in the wash from the interlayer ion exchange reactions. Another possibility is that both potassium and the divalent exchange cations randomly occupy the interlayer gallery. Assuming that a single cation per stoichiometric A-site ion (for a Dion−Jacobson phase) is necessary for the topochemical collapse to occur, only $n/2$ (n = number of unexchanged K^+ per formula unit) potassium ions are required to fill all of the A sites, leaving extra potassium that is not accounted for. While each of these scenarios could be partially correct, the most reasonable explanation is that regions of unexchanged $K_2Eu_2Ti_3O_{10}$ remain and do not topochemically collapse. Evidence for this is provided by XRD, which shows weak impurity peaks consistent with the noncollapsed layered structure of $K_2Eu_2Ti_3O_{10}$. The impurity peaks have significant line broadening, which could indicate the presence of small regions of the unexchanged phase among the collapsed exchanged phase. EDAX confirms that, even after thorough washing to remove any soluble alkali impurity, the residual potassium is present in the final ABO_3 perovskite phase.

Structural Description of New Perovskite Phases. $CsEu_2Ti_2NbO_{10}$ is structurally identical to $CsLa_2Ti_2NbO_{10}$, where Cs lies in the pocket between perovskite blocks that are stacked directly on top of each other.[29] The smaller Na and Li ions fit

Table 2. Colors and Lattice Parameters[a]

compound	color	*a*, Å	*c*, Å
$K_2Eu_2Ti_3O_{10}$	white	3.8215(3)	29.505(4)
$K_2Eu_2Ti_3O_{10}\cdot 2H_2O$	white	3.8072(2)	16.663(2)
$CsEu_2Ti_2NbO_{10}$	white	3.8087(2)	15.203(2)
$CaEu_2Ti_3O_{10}$	white	3.7854(3)	14.107(5)
$CaEu_2Ti_3O_9$	black	3.8763(2)	11.6901(9)
$SrEu_2Ti_3O_{10}$	white	3.785(2)	14.20(2)
$SrEu_2Ti_3O_9$	black	3.8830(1)	11.7056(6)
$LiEu_2Ti_2NbO_{10}$	white	3.776(1)	28.01(1)
$LiEu_2Ti_2NbO_9$	black	3.9195(1)	
$NaEu_2Ti_2NbO_{10}\cdot xH_2O$	white	3.7971(3)	34.067(5)
$NaEu_2Ti_2NbO_9$	black	3.9191(1)	
$NiEu_2Ti_3O_{10}$	lt. green	3.7679(9)	14.197(8)
$NiEu_2Ti_3O_9$	black	3.9019(3)	
$CuEu_2Ti_3O_{10}$	lt. brown/green	3.7791(6)	14.190(9)
$CuEu_2Ti_3O_9$	black	3.8790(3)	
$ZnEu_2Ti_3O_{10}$ ($ZnCl_2$)	white	3.7729(9)	27.09(2)
$ZnEu_2Ti_3O_9$ ($ZnCl_2$)	black	3.9079(3)	
$ZnEu_2Ti_3O_{10}$ (aq)	white	3.772(1)	14.57(1)
$ZnEu_2Ti_3O_9$ (aq)	black	3.9010(1)	

[a] Standard deviations are given in parentheses.

best in a smaller pocket, so the perovskite slabs in $AEu_2Ti_2NbO_{10}$ are staggered by *a*/2. The result is a change in space group from *P*4/*mmm* for $CsEu_2Ti_2NbO_{10}$ to *I*4/*mmm* for $AEu_2Ti_2NbO_{10}$ (A = Na, Li). $NaEu_2Ti_2NbO_{10}$ hydrates on exposure to air, whereas the Li compound remains anhydrous.

As expected, $K_2Eu_2Ti_3O_{10}$ and $K_2Eu_2Ti_3O_{10}\cdot 2H_2O$ are isostructural with the corresponding La compounds.[14,27] The anhydrous form has *I*4/*mmm* symmetry, while the hydrate adopts the eclipsed *P*4/*mmm* symmetry. All of the aqueous divalent ion exchanges result in similar *P*4/*mmm* (eclipsed) Dion−Jacobson structures. Interestingly, $ZnEu_2Ti_3O_{10}$ ion-exchanged in molten $ZnCl_2$ retains the *I*4/*mmm* symmetry of its Ruddlesden−Popper parent phase, whereas the aqueous exchange product shifts to *P*4/*mmm*. It is likely that the intercalation of H_2O during the aqueous ion exchange opens the interlayer galleries sufficiently far to allow lateral mobility of the perovskite slabs, which move to adopt the more stable eclipsed conformation. The $AEu_2Ti_2NbO_{10}$ (A = Na, Li) compounds were also ion-exchanged in molten salts rather than in aqueous solution, and also adopt *I*4/*mmm* structures.

Lattice parameters as determined by profile fitting using GSAS are shown in Table 2. The lattice parameters for $CsEu_2Ti_2NbO_{10}$ and $K_2Eu_2Ti_3O_{10}$ and its hydrate are somewhat smaller than those of the La analogues,[14,29] reflecting the smaller size of the Eu^{3+} ion relative to La^{3+}. The $AEu_2Ti_2NbO_{10}$ (A = Na, Li) compounds show a small decrease in the *a*-parameter due to size differences, and the perovskites $AEu_2Ti_2NbO_9$ (A = Na, Li) have nearly identical lattice parameters, since the unit cell is defined by the presence of the large Eu^{2+} ion that occupies two-thirds of the A-sites. The lattice parameters for $SrEu_2Ti_3O_{10}$ are slightly larger than those for $CaEu_2Ti_3O_{10}$ as expected, and the *a*-parameters for $SrEu_2Ti_3O_9$ and $CaEu_2Ti_3O_9$ increase by 2.5% relative to $A^{II}Eu_2Ti_3O_{10}$ to accommodate the larger Eu^{2+} ion. The *c*/*a* ratios for $A^{II}Eu_2Ti_3O_9$ (A = Ca, Sr) remain nearly identical (ca. 3.015). The lattice parameters for $M^{II}Eu_2Ti_3O_{10}$ and $M^{II}Eu_2Ti_3O_9$ are consistent with the size variation among Ni^{2+}, Cu^{2+}, and Zn^{2+}.

It is well-known that both Ti and Nb can become mixed-valent in the chemical reduction of perovskites and layered perovskites,[21b,c,30] although not nearly as easily as Eu^{3+}. While we suspect that all of the Eu^{3+} was reduced to Eu^{2+}, we cannot overlook the possibility that some Ti^{4+} and Nb^{5+} were reduced to Ti^{3+} and Nb^{4+}, respectively. Assuming that all of the Eu^{3+} was reduced, additional mixed valency of Ti and Nb would create small numbers of oxygen vacancies in the perovskite lattice that would be difficult to detect by powder XRD. It is worth noting that $KLa_2Ti_2NbO_{10}$ and $KCa_2Nb_3O_{10}$ were reduced in hydrogen under the same conditions used to form the three-dimensional perovskites, and no structural change was apparent by powder XRD. The powders turned from white to light gray, indicating that a small fraction of the Ti or Nb was reduced. This is in contrast to the samples containing Eu, which turned black upon reduction.

SEM Investigation of Particle Morphology. $CsEu_2Ti_2NbO_{10}$ and $K_2Eu_2Ti_3O_{10}$ are highly anisotropic and crystallize as flat platelets that range in size from 0.5 to 10 μm in diameter (Figure 6a). The divalent ion-exchange reactions preserve the platelet morphology of the precursors (Figure 6b). Figures 5c and 5d show that the particles remained highly textured after the hydrogen reduction. In contrast, the same compounds synthesized directly from the oxides and carbonates in hydrogen form a mixture of products including $SrTiO_3$-type perovskites that are cation-disordered (or that contain only Eu and no other A-site cations), and their particles are smaller and cubic in shape (Figure 6e). Again, this striking difference in texture provides evidence of the topochemical nature of the reaction. If the lamellar precursors had decomposed during the reduction reaction, the particle morphology would likely have changed to that of the same compounds synthesized directly under hydrogen. Also, decomposition phases would have been evident by XRD. Referring again to the progression of diffraction patterns shown in Figure 5, there is no evidence that any decomposition or dissolution of the precursor compounds occurs prior to product formation.

Conclusions

In this paper, we have demonstrated the first example of a topochemical route to three-dimensional perovskites from layered precursors. The selection of the interlayer cation determines whether the structure will be ordered or disordered. Ideally, any cations that can be incorporated into the interlayer gallery of the Dion−Jacobson and Ruddlesden−Popper precursors can be included in the three-dimensional perovskite. Ions that are normally too small to fit into the perovskite A site, or ions that typically favor a structure other than perovskite, could possibly be trapped in a perovskite lattice through this topochemical method. Also, the extension of this chemistry to include other reducible A-site or B-site ions could lead to interesting new metastable materials.

This reaction adds to a growing toolbox of topochemical transformations of perovskite-type compounds. Recently, Gopalakrishnan and co-workers have shown that Ruddlesden−Popper phases can be converted to Aurivillius phases by ion exchange intercalation,[31] and Sugahara et al. have converted Aurivillius phases back into lamellar perovskites.[32] Wiley et al. have used similar techniques to make interesting perovskite−copper halide intergrowths.[33] When these methods are combined with layer-by-layer deposition techniques,[24] it is obvious that many intergrowths and anisotropic textures of three-dimensional

(29) Gopalakrishnan, J.; Uma, S.; Bhat, V. *Chem. Mater.* **1993**, *5*, 132.
(30) Armstrong, A. R.; Anderson, P. A. *Inorg. Chem.* **1994**, *33*, 4366.
(31) Gopalakrishnan, J.; Sivakumar, T.; Thangadurai, V.; Subbanna, G. N. Submitted for publication.
(32) Sugimoto, W.; Shirata, M.; Sugahara, Y.; Kuroda, K. *J. Am. Chem. Soc.* **1999**, *121*, 11601.
(33) Kodenkandath, T. A.; Lalena, J. N.; Zhou, W. L.; Carpenter, E. E.; Sangregorio, C.; Falster, A. U.; Simons, W. B., Jr.; O'Connor, C. J.; Wiley, J. B. *J. Am. Chem. Soc.* **1999**, *121*, 10743.

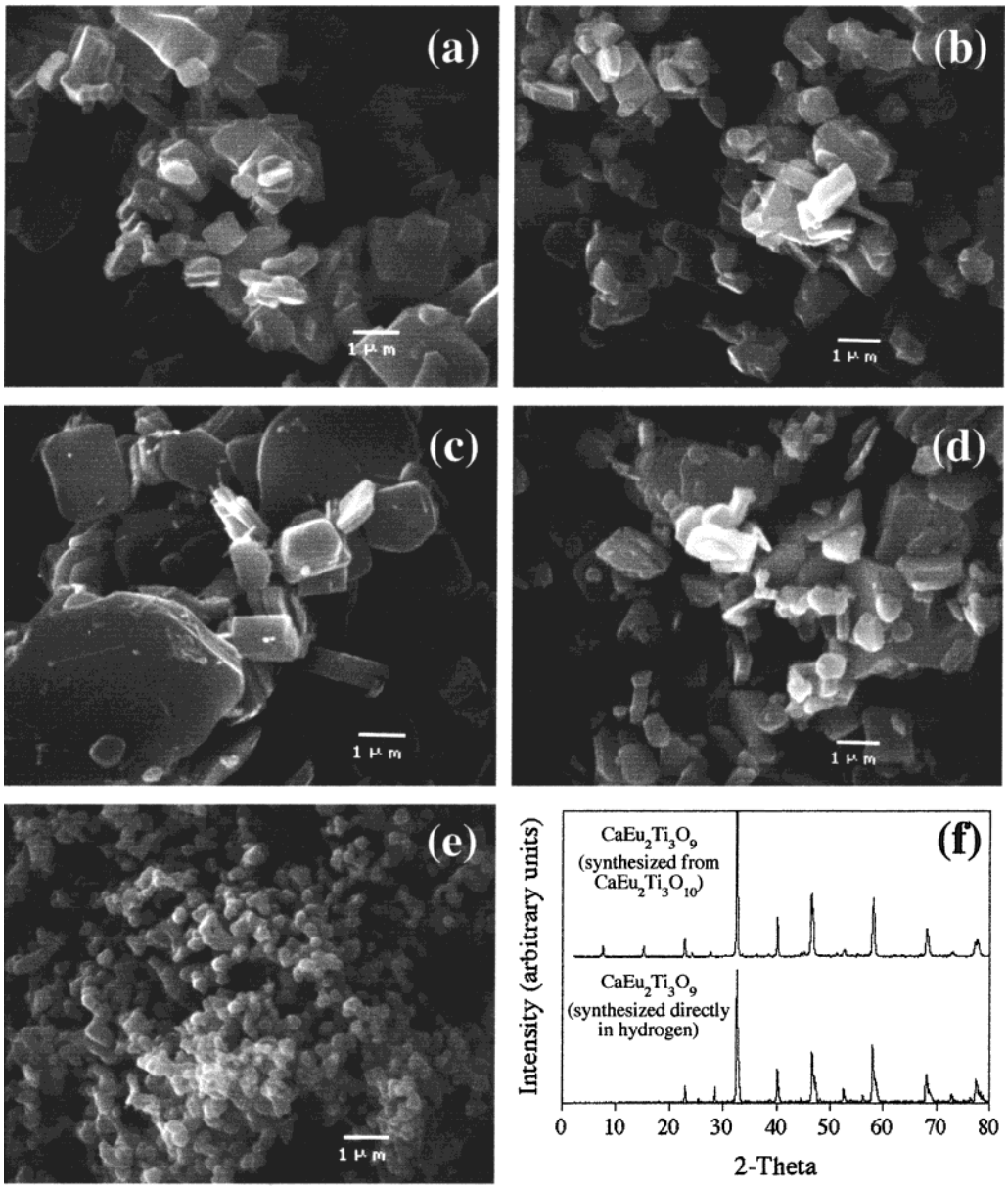

Figure 6. SEM images of (a) $K_2Eu_2Ti_3O_{10}$, (b) $CaEu_2Ti_3O_{10}$, (c) $CaEu_2Ti_3O_9$, (d) $ZnEu_2Ti_3O_9$ prepared from molten $ZnCl_2$, and (e) $CaEu_2Ti_3O_9$ prepared directly from the oxides and carbonates in hydrogen. XRD patterns for $CaEu_2Ti_3O_9$ synthesized directly and from $CaEu_2Ti_3O_{10}$ are shown in panel f.

perovskites should be possible. In this regard, one of the outstanding remaining challenges is to restack the "deck" of exfoliated Dion−Jacobson sheets with in-plane orientational order, so that the transformation to three-dimensionally ordered perovskites is possible. Research along these lines is currently in progress.

Acknowledgment. This work was supported by National Science Foundation grant CHE-9529202. This material is based upon work supported under a National Science Foundation Graduate Fellowship.

JA993306I